

Nondestructive and noncontact method for determining the spring constant of rectangular cantilevers

Dmytro S. Golovko

Max Planck Institute for Polymer Research, Ackermannweg 10, 55128 Mainz, Germany

Thomas Haschke and Wolfgang Wiechert

Department of Simulation, University of Siegen, Am Eichenhang 50, 57076 Siegen, Germany

Elmar Bonaccorso^{a)}

Max Planck Institute for Polymer Research, Ackermannweg 10, 55128 Mainz, Germany

(Received 11 January 2007; accepted 5 March 2007; published online 12 April 2007)

We present here an experimental setup and suggest an extension to the long existing added-mass method for the calibration of the spring constant of atomic force microscope cantilevers. Instead of measuring the resonance frequency shift that results from attaching particles of known masses to the end of cantilevers, we load them with water microdrops generated by a commercial inkjet dispenser. Such a device is capable of generating drops, and thus masses, of extremely reproducible size. This makes it an ideal tool for calibration tasks. Moreover, the major advantage of water microdrops is that they allow for a nearly contactless calibration: no mechanical micromanipulation of particles on cantilevers is required, neither for their deposition nor for removal. After some seconds the water drop is completely evaporated, and no residues are left on the cantilever surface or tip. We present two variants: we vary the size of the drops and deposit them at the free end of the cantilever, or we keep the size of the drops constant and vary their position along the cantilever. For the second variant, we implemented also numerical simulations. Spring constants measured by this method are comparable to results obtained by the thermal noise method, as we demonstrate for six different cantilevers. © 2007 American Institute of Physics. [DOI: 10.1063/1.2720727]

I. INTRODUCTION

Despite a number of methods for the calibration of the spring constant of atomic force microscope (AFM) cantilevers exist, there is still a need for a simple, fast, and above all contamination-free procedure, suited to different types of cantilevers. At least four calibration methods have taken root, and they are described in a series of reviews.¹⁻³ The first method is based on geometric and material properties of the cantilever (dimensions, density, and Young's modulus) together with the experimentally measured resonance frequency and quality factor, plus the viscosity and density of the medium in which the cantilever is immersed.⁴⁻⁸ This approach is suitable for rectangular cantilevers, whose dimensions are known, and shows good results (std. dev. <10%). The second method is more precise and based on the acquisition of the cantilever's thermal noise spectrum.^{9,10} It can be used for any type of cantilevers, but it is affected by one drawback: at least one force-distance curve against a hard surface has to be acquired in order to calibrate the spectrum. This often causes damage and/or contamination to the tip of the cantilever. The third method represents so-called direct techniques, where known forces are applied to the cantilever: these might be a known hydrodynamic drag at the end of the cantilever¹¹⁻¹³ or along it,¹⁴ the loading with a second cantilever of known force constant,^{15,16} the exertion

of a known electrostatic force,¹⁷ and the bombardment with drops of known mass and velocity.^{18,19} In nearly all these cases a specially developed instrument is required. One also should take into account that contamination and damage of the tip can most likely occur during the calibration while pressing the cantilever towards a reference surface. The fourth method, and the most cited/used according to ISI-Web of ScienceSM, which allows for an absolute and extremely precise calibration was proposed by Cleveland *et al.*²⁰ The idea is to measure the shift of the resonance frequency of a cantilever after loading it at its end with small, known masses. This technique, called added-mass method, works with all types of cantilevers and suffers from no restrictions, except that the mass must be placed at the very end of the cantilever and that it is time demanding.

- (i) Different particles with known mass or density must be carefully positioned onto the cantilever without contaminating it or damaging its tip;
- (ii) the thermal noise spectrum has to be recorded for each particle;
- (iii) the particles must be removed, without damaging the cantilever, and placed onto a sample holder; and
- (iv) must be later characterized in an electron microscope.

The technique would profit if some of the steps could be simplified or shortened. Motivated by this issue we have looked for a potential extension to this long established method, and we have used water microdrops instead of par-

^{a)} Author to whom correspondence should be addressed; electronic mail: bonaccur@mpip-mainz.mpg.de

ticles to load cantilevers with small masses. Two advantages are expected from this approach: first, we avoid contamination by working “contactless,” in the sense that we shoot a water drop onto the cantilever from a certain distance using an inkjet dispenser; second, since the drop evaporates after some seconds, we do not need to remove the mass “by hand.”^{18,21}

We pursued two paths to verify the validity of our technique: (i) we deposited microdrops with different sizes at the cantilever end (similar to the added-mass method) and compared the results with the predictions from beam theory, and (ii) we deposited microdrops of equal sizes at different positions along the cantilever and compared the results with the predictions of finite element method (FEM) simulations.

II. THEORY

At first, it can be instructive to mention the three time intervals into which a drop impact on a solid surface is divided.^{18,22,23} In the beginning the drop hits the solid surface and spreads until it has reached its maximal contact radius and takes the shape of a spherical cap. This spreading process is characterized by a time constant τ_s of about 1 ms for drops with a radius between 10 and 30 μm . The impact of the drop causes the cantilever to oscillate. The initial oscillation is damped, and the amplitude decays exponentially with a time constant τ_d , which we measured to be between 2 and 10 ms in air. Finally, the drop evaporates from the cantilever and the time τ_e it takes is on the order of 1 s. Practically, we are interested in the second time domain τ_d , which is well separated from the other two, and is long enough to record the oscillations of the cantilever with a good time resolution. During τ_d the mass of the drop does not significantly change due to evaporation.²⁴ When a drop of mass m hits the cantilever with a velocity v_0 at $t=0$ we assume that its momentum is effectively transferred. The cantilever starts to oscillate until damping brings it to rest again. This process can be described by the equation of motion, assuming that no external forces are acting and neglecting gravitation,

$$m^* \frac{d^2 z}{dt^2} + D \frac{dz}{dt} + Kz = 0. \quad (1)$$

Here, z is the deflection of the cantilever, D is a damping coefficient, m^* is the effective mass, and K is the spring constant of the cantilever. Equation (1) is valid for the deflection of the cantilever at its end and is independent of its form. For the special case of a rectangular cantilever, the spring constant is

$$K = \frac{Ewd^3}{4l_0^3}, \quad (2)$$

where E is Young’s modulus of the material, w is the width, d the thickness, and l_0 the length of the cantilever.

The effective mass is

$$m^* = m + aM, \quad (3)$$

where m is the mass of the drop, M is the mass of the cantilever, and a is a form factor. For rectangular cantilevers $a=0.243$. We ideally assume that the drop is positioned at the free end of the cantilever and that the cantilever oscillates in

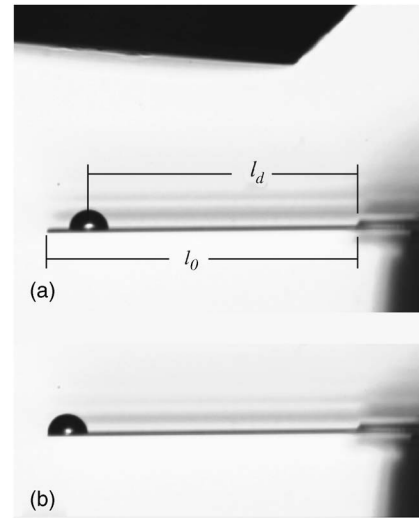


FIG. 1. A microdrop of water close to (A) and at the end (B) of a rectangular silicon cantilever, directly after impact.

its first oscillation mode (for details, see Refs. 9 and 25). The general solution of Eq. (1) is

$$z(t) = -A_0 \sin(\omega t + \varphi) e^{-t/\tau_d}, \quad (4)$$

with

$$\omega = 2\pi f = \sqrt{\frac{K}{m^*}} \quad (5)$$

and $\tau_d = 2m^*/D$. Initially, the deflection of the cantilever is zero, $z(t=0)=0$, which leads to $\varphi=0$. The negative sign in Eq. (4) takes into account that the falling drop causes the cantilever first to bend downward. Combining Eqs. (3) and (5), we can calculate the spring constant from the initial resonance frequency of the cantilever with the drop,

$$f = \frac{1}{2\pi} \sqrt{K/(m + aM)}, \quad (6)$$

and the resonance frequency without the drop,

$$f_0 = \frac{1}{2\pi} \sqrt{\frac{K}{aM}} = \frac{1}{4\pi} \frac{d}{l_0^2} \sqrt{\frac{E}{a\rho}}, \quad (7)$$

where ρ is the density of the material.

Rearranging Eq. (6) one obtains

$$m = K \frac{1}{(2\pi f)^2} - aM. \quad (8)$$

Equation (8) shows that if several drops of known masses are placed at the free end of a cantilever and the respective resonance frequencies are measured, a linear plot of drop masses versus $(2\pi f)^{-2}$ should give a straight line, the slope being the spring constant and the negative Y -axis intercept the effective mass. This makes the method similar to the one proposed by Cleveland *et al.*²⁰ So far we discussed the ideal case of a mass placed at the very end of a cantilever. However, this can hardly be achieved in experimental practice. Figure 1(a) shows a rectangular silicon cantilever with a water drop on it, directly after impact. Like represented in the figure, the rim of the drop is at a certain distance from the free end of the cantilever. Nonetheless, also if we place the

drop at the end [Fig. 1(b)], due to the spatial extension of the drop, its radius determines the distance of the center of mass. We must take this into account by considering the dependency of the spring constant on the position of the center of mass. For small distances this dependency can be approximated by

$$\frac{K}{l_0^3} = \frac{K_d}{l_d^3}. \quad (9)$$

K_d is the measured spring constant for a drop of mass m_d , with its center of mass located at l_d from the base of a cantilever that has an overall length l_0 . K is then the spring constant if the same drop would have its center of mass located at the very end. We used Eq. (9) for calculating the spring constants of all examined cantilevers.

For larger distances the approximation given by Eq. (9) is not valid anymore. Moreover, it is not possible to find an analytic solution for the equation of motion of a cantilever with a drop deposited at an arbitrary position along its length axis different from the very end. The alternative is to use numerical simulations. To this purpose, a numerical three-dimensional (3D) model is implemented and solved by means of the FEM software package COMSOL Multiphysics.^{19,26} This model, contrary to beam theory, takes into account Poisson's ratio ν of the cantilever material,¹⁹ which for silicon is around 0.26. For reasons of simplicity instead of a spherical drop we used an equivalent cylindrical drop having similar mass. The dimensions of the cylinder are calculated from the drop mass m and the contact radius a , which are known from video analysis. We set the radius of the cylinder a_{cyl} equal to the contact radius of the drop and calculated the height h_{cyl} by

$$h_{\text{cyl}} = \frac{m}{a_{\text{cyl}} \rho_d \pi}, \quad (10)$$

with ρ_d the density of the drop. The center of mass of cylinder and drop are the same. The cantilever with its known material properties (E , ν , and ρ) and dimensions (l_0 , w , and d) is modeled as a cuboid clamped on one side.

The simulation typically comprises about 10.000 elements and about 60.000 degrees of freedom using an unstructured tetrahedron mesh. In order to improve the numerical accuracy the initial mesh was automatically refined two times. The model was validated by comparing the simulated resonance frequencies of the loaded as well as of the unloaded cantilevers with the resonance frequencies measured in the experiments.

With this so called "forward simulation" we can confirm the experimental method, i.e., calculate the resonance frequency using parameters of the cantilever (E , ν , ρ , l_0 , w , and d) known *a priori*. On the other hand, one could use an "inverse simulation" to determine unknown parameters which are experimentally hardly accessible. We could thus solve the inverse problem of identifying the cantilever's thickness with respect to a given resonance frequency f_i by inserting the other parameters (E , ν , ρ , l_0 , w , and f_i) into an optimization routine for obtaining the thickness by minimizing the error between simulated and measured resonance frequencies. The optimization routine is stopped when the error

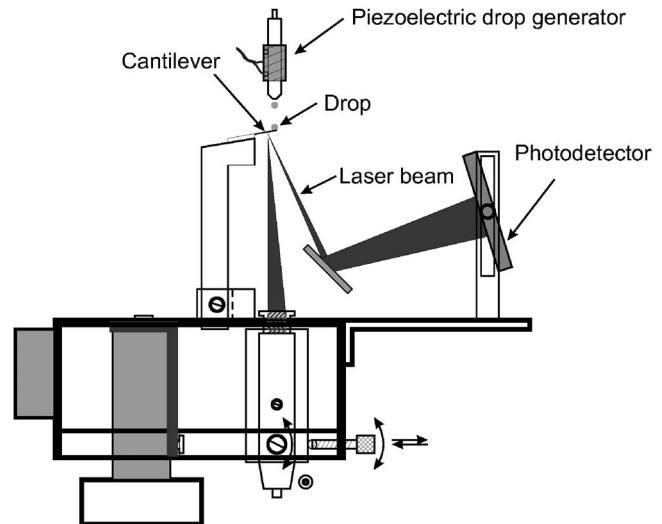


FIG. 2. Experimental setup for spring constant calibration using microdrops of different masses. The drop is generated by an inkjet dispenser and impacts on the cantilever from above. The deflection of the cantilever is measured with a laser from below with the light lever technique and with a photodetector. The camera with the zoom optics is directed perpendicularly to the plane of the figure.

is below 0.1%. The inverse problem is solved for the unloaded cantilever and for each configuration where a drop is sitting at a different position along the cantilever. Then the mean value of all obtained thicknesses is inserted into Eq. (2) to calculate the spring constant of the cantilever.

III. MATERIALS AND METHODS

Figure 2 shows the experimental setup, a reversed particle interaction apparatus (R-PIA),^{18,27} which we used to deposit microdrops on cantilevers, to measure cantilever oscillations after the impact, and to measure the position of the drops along the cantilever. Water drops of diameters between 10 and 65 μm (milliQ, Millipore Corp., Bedford, MA) were generated by a software-controlled piezoelectric droplet generator²⁸ (Piezodropper, Universität Bremen, Germany). Each drop is produced at a distance of ≈ 0.2 mm from the cantilever surface. By varying the impulse duration and the voltage applied to the piezodropper we controlled the drop diameters. A three-axis, electromotor-controlled micromanipulator (Luigs & Neumann GmbH, Ratingen, Germany) was used for depositing the drops on the desired place on a horizontally mounted micromachined cantilever ("octosensis" rectangular silicon cantilevers from Micromotive GmbH, Mainz, Germany; rectangular silicon cantilevers from Nanosensors, Neuchâtel, Switzerland; triangular silicon nitride cantilevers from Veeco Instruments, Santa Barbara, CA). Dimensions and properties of the cantilevers are given for each experiment and summarized in Table I. Cantilever spring constants and their unloaded resonance frequencies were calibrated with the MFP-ID (Asylum Research, Santa Barbara, CA) by the thermal noise (TN) method.^{9,10} With these reference values we then compared the results of our calibration.

The deposition of a drop on the free end of the cantilever causes the cantilever to oscillate. This oscillation is measured

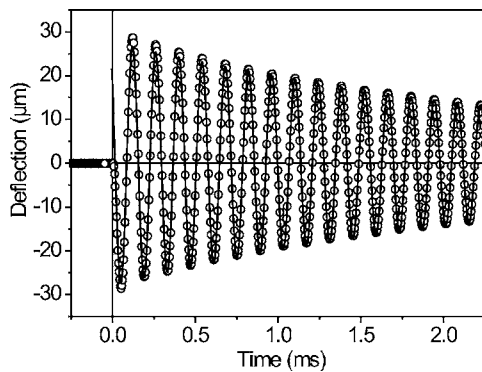


FIG. 3. Cantilever deflection vs time after drop impact. Drop properties: initial mass $m_i=68.3$ ng, $R=25.37$ μm , velocity $v_0=2.2$ m/s. Cantilever properties: $l_0=500$ μm , $w=90$ μm , $d=1.89$ μm . Negative deflection indicates that the cantilever is bent downward. Open circles (O) represent the oscillating cantilever deflection. The solid line represents a fit of Eq. (4) to the experimental data points ($A_0=27.9$ μm , $f_i=7114$ Hz, $\tau_d=2.98$ ms).

by the light lever technique commonly employed in AFM, pointing a laser beam on the backside of the cantilever, at a position between the drop and the base of the cantilever (see Fig. 2), and measuring the position of the reflected beam with a photodetector. Cantilever deflections during oscillation could be measured with nanometer accuracy. To visualize the deposition process the position and the contours of the drops were monitored with a camera system consisting of an objective $5\times$ (Mitutoyo Corp., Kawasaki, Japan), a $6.5\times$ Ultra zoom tube (Navitar Inc., Rochester, NY), and a uEye UI-2210-C, charge coupled device (CCD) camera (IDS GmbH, Obersulm, Germany), together with a white light source (Schott KL 1500, Mainz, Germany). The resolution of a single frame was 640×480 pixels; the frame rate was 25 fps (frames per second). From video images, the contact radius and height of the drops were obtained. From the first frame in each video sequence, as a drop appears, we calculated the contact radius a and the height h of the drop cap. To know $\mu\text{m}/\text{pixel}$ ratio the system was previously calibrated using a cantilever with a known length. From a and h , the

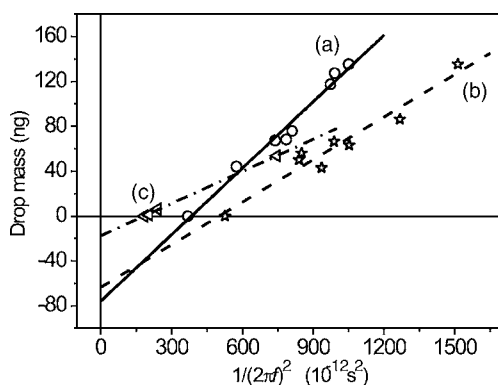


FIG. 4. Plots of different water drop masses vs $1/(2\pi f)^2$ according to Eq. (9) for three cantilevers. (A) Rectangular cantilever: $l_0=500$ μm , $w=90$ μm . A linear regression of the data yields effective mass=75.9 ng, $K=0.198\pm 0.012$ N/m. (B) Rectangular cantilever: $l_0=460$ μm , $w=50$ μm . Effective mass=63.4 ng, $K=0.126\pm 0.012$ N/m. (C) Triangular cantilever: $l_0=200$ μm , $w=22$ μm . Effective mass=17.6 ng, $K=0.096\pm 0.002$ N/m.

drop volume was calculated by $V=\pi h(3a^2+h^2)/6$. The drop deposition took place at a temperature of $22(\pm 1)^\circ\text{C}$ and a relative humidity of $40(\pm 5)\%$.

IV. RESULTS AND DISCUSSION

A typical experimental cantilever deflection versus time curve after drop impact and a fit of the curve with Eq. (4) are shown in Fig. 3. The cantilever is at rest for $t<0$, it is excited at $t=0$ and it starts to oscillate, and it is damped for $t>0$ until the resting position is again attained. We performed three series of experiments using different cantilevers and drops (see also Table I).

- (A) Rectangular Micromotive cantilever with $f_0=10\,404$ Hz and $K_{\text{TN}}=0.19\pm 0.01$ N/m, seven drops, masses varied from 44.2 ng ($R=21.95$ μm) to 135.4 ng ($R=31.88$ μm).
- (B) Rectangular Nanosensors cantilever with $f_0=11\,782$ Hz and $K_{\text{TN}}=0.13\pm 0.01$ N/m, seven drops, masses varied from 43.1 ng ($R=21.76$ μm) to 135.5 ng ($R=31.88$ μm).
- (C) Triangular Veeco cantilever with $f_0=19\,253$ Hz and $K_{\text{TN}}=0.10\pm 0.01$ N/m, three drops, masses varied from 1.1 ng ($R=6.41$ μm) to 53.7 ng ($R=23.41$ μm).

According to Eq. (8), which establishes the relation between the deposited mass and the resulting resonance frequency of the cantilever, we show the results of the three series of measurements in Fig. 4. We also included the unloaded resonance frequencies of cantilevers in the data sets ($m=0$). The relation between the drop mass m and $1/(2\pi f)^2$ is linear, as expected, and the slopes of the fitted lines provide the spring constants: $K_{\text{experiment(A)}}=0.198\pm 0.012$ N/m, $K_{\text{experiment(B)}}=0.126\pm 0.012$ N/m, and $K_{\text{experiment(C)}}=0.096\pm 0.002$ N/m. All these values differ by less than 5% from the values obtained by the TN method and confirm the validity of the technique. Moreover, no residues are left on the cantilever, which means that the AFM probe has not been corrupted or contaminated during calibration.

As we have seen drop sizes can be varied by the piezo-control parameters, but this is time demanding: the drop size strongly depends on the inner diameter of the nozzle, which is fixed, and operating on the piezocontrols allows us to vary the drop diameter by at most an order of magnitude. This does provide only a limited spectrum of masses to be used for calibration. An alternative to changing drop sizes is to use the inkjet dispenser for generating monodisperse droplets (according to the manufacturer, the standard deviation of the drop diameters is less than 1%), and to deposit them at different positions along the length axis of the cantilever. Other than the previous technique, this is applicable only to rectangular cantilevers. The loads sensed by the cantilever are different, and so will be the shifts of the resonance frequencies with respect to the unloaded cantilever. Results of such experiments are presented in Fig. 5: we deposited drops of similar mass on three rectangular silicon cantilevers, all having the same width and only slightly different thicknesses, but distinct lengths and thus resonance frequencies. We de-

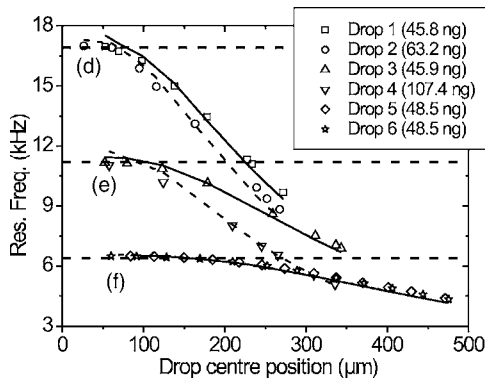


FIG. 5. Resonance frequency vs drop center position for three rectangular cantilevers. Cantilever properties: (D) $l_0=297 \mu\text{m}$, $w=90 \mu\text{m}$, $d=1.05 \mu\text{m}$, $K_{\text{TN}}=0.178\pm 0.01 \text{ N/m}$. (E) $l_0=372 \mu\text{m}$, $w=90 \mu\text{m}$, $d=1.09 \mu\text{m}$, $K_{\text{TN}}=0.104\pm 0.01 \text{ N/m}$. (F) $l_0=503 \mu\text{m}$, $w=90 \mu\text{m}$, $d=1.18 \mu\text{m}$, $K_{\text{TN}}=0.053\pm 0.005 \text{ N/m}$. Different drop masses used for each cantilever are shown on the figure. Experimental data points are represented by hollow symbols, simulations by solid lines. The horizontal dashed lines represent the three unloaded resonance frequencies as measured by the TN method.

terminated the spring constants by the TN method, and the average thickness d of the cantilevers with Eq. (2) (see also Table I).

- (D) $l_0=297 \mu\text{m}$, $K_{\text{TN}}=0.178\pm 0.01 \text{ N/m}$, $d=1.05 \mu\text{m}$.
 (E) $l_0=372 \mu\text{m}$, $K_{\text{TN}}=0.104\pm 0.01 \text{ N/m}$, $d=1.09 \mu\text{m}$
 (F) $l_0=503 \mu\text{m}$, $K_{\text{TN}}=0.053\pm 0.003 \text{ N/m}$, $d=1.18 \mu\text{m}$

For each cantilever we performed two series of experiments, each one with a different load (54 experimental configurations in total). In fact, drops of different masses located at the same position cause different frequency shifts, as is demonstrated, e.g., by drops 3 and 4. Furthermore, an evaluation of the curves in Fig. 5 confirms what we mentioned before, i.e., that the relationship between drop position and resonance frequency is not linear. Since it is not possible to find an analytic solution analog to Eq. (6) for these types of “cantilever-mass” configuration, we had to simulate them (continuous lines in Fig. 5). The very good agreement between experiments and simulations makes the presented technique an interesting alternative to the added-mass method: the number of masses we can deposit is sufficiently large for any type of statistics (the error coming from the uncertainty in determining the exact position of the drops from the video images is counterbalanced by the large number of drops that can be deposited), and the reproducibility of

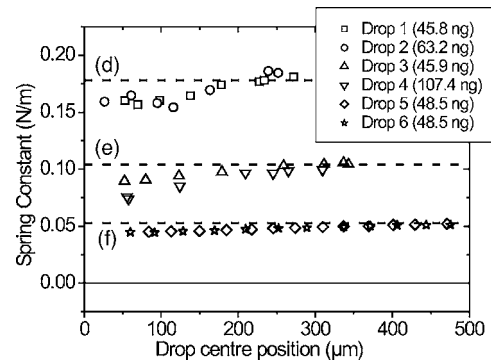


FIG. 6. Spring constants of cantilevers (D), (E), and (F), plotted vs drop center position. Spring constants determined by the TN method are plotted as horizontal dashed lines, while the mean value of the spring constants determined with the drop method are, respectively, $K_{\text{experiment}}=0.170\pm 0.010 \text{ N/m}$, $0.098\pm 0.006 \text{ N/m}$, and $0.048\pm 0.002 \text{ N/m}$.

the drop mass is very good (see masses of drops 5 and 6 in Fig. 5, e.g., noting that the two curves were acquired at different times).

Moreover, the whole procedure is automated: after having determined the size of the drops, we set the positions where we want to deposit them and we decide the number of cycles we want to run for each cantilever. Then we start the data acquisition and record the resonance frequencies (curves like they are sketched in Fig. 5) and the contact radii. With these values, we start the automated inverse simulation cycle and identify the cantilevers’ thickness for each of the 54 data points. Next the mean thickness of each cantilever is calculated and inserted into Eq. (2). The results are the spring constants corresponding to each single data point, as shown in Fig. 6. The results of the 54 simulated configurations differ for all data points by less than 6% from the experimental data, and only in one case the relative error is around 10%. This is also the expected error range of the calibration with the TN method.

Inspection of the spring constant data presented in Fig. 6 suggests that there is a systematic error, leading to a slope in the determined data points with the position of the drop center. We do not have an explanation for this yet; however, we can exclude some facts and speculate on some others. We performed a parameter study with Poisson’s ratio and can thus exclude its influence. The magnitude of the simulated spring constant slightly changed, being largest for smallest Poisson’s ratio, but the magnitude of the slope remained

TABLE I. The six types of calibrated cantilevers, with spring constants measured according to the thermal noise (TN) and to the drop (experiment) method, and the relative error.

Cantilever type	l_0 (μm)	f_0 (Hz)	K_{TN} (N/m)	No. of drops	$K_{\text{experiment}}$ (N/m)	E_{rel} (%) $(K_{\text{TN}}-K_{\text{experiment}})/K_{\text{TN}}$
(A) Micromotive, rect.	500	10 404	0.19 ± 0.01	7	0.198 ± 0.012	4.2
(B) Nanosensors, rect.	460	11 782	0.13 ± 0.01	7	0.126 ± 0.012	3.1
(C) Veeco, triang.	200	19 253	0.10 ± 0.01	3	0.096 ± 0.002	4.0
(D) Micromotive, rect.	297	16 900	0.178 ± 0.01	2×8	0.170 ± 0.010	4.5
(E) Micromotive, rect.	372	11 215	0.104 ± 0.01	2×7	0.098 ± 0.006	5.8
(F) Micromotive, rect.	503	6 400	0.053 ± 0.01	2×12	0.048 ± 0.002	9.4

nearly unaffected. We therefore chose $\nu=0.26$, since it is a standard value from literature for crystalline silicon. We can also exclude the effect of the transversal bending of the cantilever caused by the drop,¹⁹ which is more pronounced when the drop is closer to the base of the cantilever, because this would cause a stiffening rather than a softening of the cantilever. More on the speculative side is that higher vibration modes are excited and become more pronounced when the drop is deposited closer to the base of the cantilever. This might be the reason of the systematic experimental error which leads to an “apparent” smaller spring constant. However, at the moment being we are not able to confirm/disprove this speculation using the simulation tools we are working with.

We presented an extension to the existing added-mass method for the calibration of AFM cantilever spring constants, and developed an experimental calibration setup and an automated simulation routine. Instead of attaching particles of known masses to the end of cantilevers and measuring the resulting resonance frequency shift, we loaded the cantilevers with water microdrops with comparable masses. The microdrops were generated by a commercial inkjet dispenser, whose principal characteristic is to produce drops of extremely reproducible size. It is thus ideal for calibration tasks. Another significant advantage of water drops is that they allow for a nearly contactless calibration: no mechanical micromanipulation of particles on cantilevers is required, neither for deposition nor for removal. After some seconds from generation, the water drop has completely evaporated, and no residues are left on the cantilever surface or tip. We applied two variants of the technique for calibrating the spring constants of six cantilevers: one by varying the drop size, and the other by varying the drop location. Both yielded results very close to the thermal noise calibration. The drop technique is practically suited for large cantilevers that are commonly used as micromechanical sensors. We have also shown, however, that with a little of experience smaller drops can be produced, enabling thus the calibration of cantilevers with dimensions around 200 μm , which are widely used in standard atomic force microscopy.

ACKNOWLEDGMENTS

The authors thank Andreas Best and Karsten Büscher for helping developing the experimental setup, Michael Kappl for assistance in programming the data acquisition software, and Hans-Jürgen Butt for helpful discussions. They acknowledge financial support from the Max Planck Society (MPG).

- ¹N. A. Burnham, X. Chen, C. S. Hodges, G. A. Matei, E. J. Thoreson, C. J. Roberts, M. C. Davies, and S. J. B. Tendler, *Nanotechnology* **14**, 1 (2003).
- ²H. J. Butt, B. Cappella, and M. Kappl, *Surf. Sci. Rep.* **59**, 1 (2005).
- ³J. Ralston, I. Larson, M. W. Rutland, A. A. Feiler, and M. Kleijn, *Pure Appl. Chem.* **77**, 2149 (2005).
- ⁴J. E. Sader, I. Larson, P. Mulvaney, and L. R. White, *Rev. Sci. Instrum.* **66**, 3789 (1995).
- ⁵J. E. Sader, *J. Appl. Phys.* **84**, 64 (1998).
- ⁶J. E. Sader, J. W. M. Chon, and P. Mulvaney, *Rev. Sci. Instrum.* **70**, 3967 (1999).
- ⁷C. P. Green, H. Lioe, J. P. Cleveland, R. Proksch, P. Mulvaney, and J. E. Sader, *Rev. Sci. Instrum.* **75**, 1988 (2004).
- ⁸M. J. Higgins, R. Proksch, J. E. Sader, M. Polcik, S. Mc Endoo, J. P. Cleveland, and S. P. Jarvis, *Rev. Sci. Instrum.* **77**, 013701 (2006).
- ⁹H.-J. Butt and M. Jaschke, *Nanotechnology* **6**, 1 (1995).
- ¹⁰J. L. Hutter and J. Bechhoefer, *Rev. Sci. Instrum.* **64**, 1868 (1993).
- ¹¹T. J. Senden and W. A. Ducker, *Langmuir* **10**, 1003 (1994).
- ¹²V. S. J. Craig and C. Neto, *Langmuir* **17**, 6018 (2001).
- ¹³S. M. Notley, S. Biggs, and V. S. J. Craig, *Rev. Sci. Instrum.* **74**, 4026 (2003).
- ¹⁴N. Maeda and T. J. Senden, *Langmuir* **16**, 9282 (2000).
- ¹⁵M. Tortonese and M. Kirk, *Proc. SPIE* **3009**, 53 (1997).
- ¹⁶A. Torii, M. Sasaki, K. Hane, and S. Okuma, *Meas. Sci. Technol.* **7**, 179 (1996).
- ¹⁷E. Bonaccorso, F. Schönfeld, and H. J. Butt, *Phys. Rev. B* **74**, 085413 (2006).
- ¹⁸E. Bonaccorso and H. J. Butt, *J. Phys. Chem. B* **109**, 253 (2005).
- ¹⁹T. Haschke, E. Bonaccorso, H.-J. Butt, D. Lautenschlager, F. Schönfeld, and W. Wiechert, *J. Micromech. Microeng.* **16**, 2273 (2006).
- ²⁰J. P. Cleveland, S. Manne, D. Bocek, and P. K. Hansma, *Rev. Sci. Instrum.* **64**, 403 (1993).
- ²¹E. Bonaccorso and G. Gillies, *Langmuir* **20**, 11824 (2004).
- ²²M. von Bahr, F. Tiberg, and B. Zhmud, *Langmuir* **19**, 10109 (2003).
- ²³A. L. Yarin, *Annu. Rev. Fluid Mech.* **38**, 159 (2006).
- ²⁴H. J. Butt, D. S. Golovko, and E. Bonaccorso, *J. Phys. Chem. B* (submitted).
- ²⁵H.-J. Butt *et al.*, *J. Microsc.* **169**, 75 (1993).
- ²⁶www.comsol.com
- ²⁷M. Preuss and H.-J. Butt, *Langmuir* **14**, 3164 (1998).
- ²⁸H. Ulmke, T. Wriedt, and K. Bauckhage, *Chem. Eng. Technol.* **24**, 265 (2001).